 CMES, vol.2, no.4, pp.423-433, 2001

A Pure Contour Formulation for the Meshless Local Boundary Integral Equation Method in Thermoelasticity

J. Sladek [1] , V. Sladek[1] and S.N. Atluri [2]

1 Abstract

A new meshless method for solving stationary thermoelastic boundary value problems is proposed in the present paper. The moving least square (MLS) method is used for the approximation of physical quantities in the local boundary integral equations (LBIE). In stationary thermoelasticity, the temperature and displacement fields are uncoupled. In the first step, the temperature field, described by the Laplace equation, is analysed by the LBIE. Then, the mechanical quantities are obtained from the solution of the LBIEs, which are reduced to elastostatic ones with redefined body forces due to thermal loading. The domain integrals with temperature gradients are transformed to boundary integrals. Numerical examples illustrate the implementation and performance of the present method.

2 Introduction

The meshless discretization approach for continuum mechanics problems has attracted much attention during the past decade [Belytschko et al.(1996); Lin and Atluri(2000); Kim and Atluri(2000); Ching and Batra(2001); and Gu and Liu(2001)]. By focusing only on the points, instead of the meshed elements as in the conventional FEM or BEM, the meshless approach has certain advantages. Nodal points are randomly spread on the domain of analysed body. Every node is surrounded by a simple surface centered at the collocation point. Only one nodal point is included into the subdomain. On the surface of subdomains the local boundary integral equations are written. Then, the number of equations is equal to number of nodes.

In the present paper, stationary thermoelastic problems are analysed. In such a case, the temperature and displacement fields are uncoupled [Balas et al.(1989)]. Then, in the first step, the temperature field is analysed. If thermal fields (temperature and heat flux) are known, the mechanical quantities (displacement and traction vector) are obtained from the solution of the local boundary integral equations, which are reduced to the elastostatic LBIE with known redefined body forces. The redefined body force is proportional to the temperature gradients. The domain integral with temperature gradients in stationary thermoelasticity can be transformed to boundary integrals [Balas et al.(1989)]. The pure local boundary integral equation formulation is computionally efficient due to avoiding domain integration.

Both displacement and traction vectors are unknown on the local boundary. If a companion solution [Zhu et al.(1998); Atluri et al.(2000)] to the Kelvin fundamental solution is introduced, in order to give a zero value of the final fundamental displacement on the local boundary, the tractions are eliminated in the LBIEs allocated to interior points. Displacements are approximated by the moving least-square (MLS) method [Belytschko et al.(1994)]. The essential idea of MLS interpolants is that it is only necessary to construct an array of nodes in the domain under consideration. The discussion devoted to the selection of two free parameters in the MLS approximation is presented via the numerical example represented by a hollow cylinder under a thermal load.

3 Local boundary integral equations in stationary thermoelasticity

Consider a homogeneous, isotropic and perfectly elastic body occupying the region Ω and bounded by the surface Γ. The governing equations in stationary thermoelasticity are given by [Balas et al.(1989)]

$$\theta_{,kk} = \frac{Q}{\kappa_0} \tag{1}$$

[1] Institute of Construction and Architecture, Slovak Academy of Sciences, 842 20 Bratislava, Slovakia

[2] Center for Aerospace Research & Education, 7704 Boelter Hall, University of California at Los Angeles, Los Angeles, CA 90095-1600, USA

$$\mu u_{i,kk} + (\lambda+\mu) u_{k,ki} + X_i = \gamma \theta_{,i} \tag{2}$$

where $\theta = T - T_0$ denotes the increase of temperature with respect to the natural state T_0 for which the stresses and deformations are equal to zero. Next, u_i and X_i denote the components of the displacement vector and the body force vector, respectively. The heat source is denoted by Q, while κ_0 is the thermal diffusivity, and the constant γ is expressed in terms of the Lame constants μ and λ as

$$\gamma = (2\mu + 3\lambda)\alpha$$

with α being the coefficient of linear thermal expansion.

It is seen that the governing equations are uncoupled and they can be solved separately. In the first step we solve the Poisson equation (1). The weak formulation of the equation can be written as

$$\int_\Omega [\theta_{,kk}(x) - Q/\kappa_0(x)]\theta^*(x) d\Omega = 0 \tag{3}$$

where $\theta^*(x)$ is the test function and $\theta(x)$ is the trial function for temperature.

Applying the Gauss divergence theorem to the first term in the in the integral given by eq. (3), we have

$$\int_\Omega \theta_{,kk}(x)\theta^*(x) d\Omega = \int_\Gamma \frac{\partial \theta}{\partial n}(x)\theta^*(x) d\Gamma - \int_\Gamma \theta(x)\frac{\partial \theta^*}{\partial n}(x) d\Gamma + \int_\Omega \theta^*_{,kk}(x)\theta(x) d\Omega \tag{4}$$

If the test function (weighting field) satisfies the following equation

$$\theta^*_{,kk}(x,y) + \delta(x,y) = 0 \tag{5}$$

where $\delta(x,y)$ is the Dirac delta function, the following integral representation for temperature can be obtained from eqs. (3) – (5)

$$\theta(y) = \int_\Gamma \frac{\partial \theta}{\partial n}(x)\theta^*(x,y) d\Gamma - \int_\Gamma \theta(x)\frac{\partial \theta^*}{\partial n}(x,y) d\Gamma - \int_\Omega \theta^*(x,y)\frac{Q}{\kappa_0}(x) d\Omega \tag{6}$$

where $\boldsymbol{n}$ is the unit outward normal vector to the boundary Γ.

The boundary integral equation (6) relates quantities (θ- temperature and $q = \partial\theta/\partial n$ heat flux) on the global boundary Γ. If, instead of the entire domain Ω of the given problem, we consider a subdomain Ω_s, which is located entirely inside Ω, the following equation should also hold over the subdomain Ω_s

$$\theta(y) = \int_{\partial\Omega_s} \frac{\partial \theta}{\partial n}(x)\theta^*(x,y) d\Gamma - \int_{\partial\Omega_s} \theta(x)\frac{\partial \theta^*}{\partial n}(x,y) d\Gamma - \int_{\Omega_s} \theta^*(x,y)\frac{Q}{\kappa_0}(x) d\Omega \tag{7}$$

where $\partial\Omega_s$ is the boundary of the subdomain Ω_s.

In the original boundary value problem, either the temperature $\theta(x)$ or the heat flux $q = \partial\theta/\partial n$ may be specified at every point on the global boundary Γ, which makes a well-posed problem. But none of them is known a priori along the local boundary $\partial\Omega_s$. To eliminate the flux variable from the integral representation (7), Atluri and his co-workers (1998) introduced a 'companion solution' to the fundamental solution in such a way that the final modified fundamental solution is zero on the circular boundary $\partial\Omega_s$. The modified fundamental solution can be easily derived for the Laplace equation and for 2-d problems is given by

$$\tilde{\theta}^*(x,y) = \frac{1}{2\pi}\ln\frac{r_0}{r} \tag{8}$$

where $r = |x-y|$ and r_0 is the radius of the local subdomain Ω_s.

Taking into account that

$$\tilde{\theta}^*(r)\big|_{r=r_0} = 0 \tag{9}$$

one can rewrite eq. (7) into the form

$$\theta(y) = -\int_{\partial\Omega_s} \theta(x)\frac{\partial\tilde{\theta}^*}{\partial n}(x,y)d\Gamma - \int_{\Omega_s} \tilde{\theta}^*(x,y)\frac{Q}{\kappa_0}(x)d\Omega \tag{10}$$

for the source point located inside Ω.

When the source point y is located on the global boundary Γ, the subdomain can still be taken as a part of a circular domain with the boundary composed of a circular part L_s and the piece of boundary line Γ_s on which the nodal point is lying $(\partial\Omega_s = L_s \cup \Gamma_s)$. It should be noted that along the line Γ_s the modified fundamental solution $\tilde{\theta}^*$ is not zero. Then, the local boundary integral equation for nodes $\zeta \in \Gamma_s \subset \Gamma$ becomes

$$\begin{aligned}\theta(\zeta) &+ \int_{L_s} \theta(x)\frac{\partial\tilde{\theta}^*}{\partial n}(x,\zeta)d\Gamma \\ &+ \lim_{y\to\zeta}\int_{\Gamma_s} \theta(x)\frac{\partial\tilde{\theta}^*}{\partial n}(x,y)d\Gamma - \int_{\Gamma_s} \tilde{\theta}^*(x,\zeta)q(x)d\Gamma = \\ &- \int_{\Omega_s} \tilde{\theta}^*(x,\zeta)\frac{Q}{\kappa_0}(x)d\Omega\end{aligned} \tag{11}$$

Although the LBIE (11) can be rewritten into a non-singular form, it is more appropriate to use this limit form because of the numerical integration when the MLS-approximation is employed [Sladek et al.(2000)].

In the second step the Lame-Navier governing equation (2) is solved. The same procedure, as in the case of the Poisson equation, is repeated. The weak formulation is given as

$$\int_\Omega [\mu u_{i,kk}(x) + (\lambda+\mu)u_{k,ki}(x) + X_i(x) - \gamma\theta_{,i}(x)]u_i^*(x)d\Omega = 0, \tag{12}$$

where $u_i^*(x)$ is a weight function.

Applying the Gauss divergence theorem to the domain integral in eq. (12), one can write

$$\begin{aligned}&\int_\Omega \left[\mu u_{i,kk}^*(x) + (\lambda+\mu)u_{k,ki}^*(x)\right]u_i(x)d\Omega \\ &\quad + \int_\Gamma [t_i(x) + \gamma n_i(x)\theta(x)]u_i^*(x)d\Gamma - \int_\Gamma t_i^*(x)u_i(x)d\Gamma \\ &\quad = \int_\Omega [\gamma\theta_{,i}(x) - X_i(x)]u_i^*(x)d\Omega\end{aligned} \tag{13}$$

where

$$t_i = \sigma_{ij}n_j = \mu u_{i,k}n_k + \lambda u_{k,k}n_i + \mu u_{k,i}n_k - \gamma\delta_{ij}n_j\theta$$

is the traction vector.

If the weight field is selected as the elastostatical fundamental solutions of the elastostatical governing equation

$$\mu U_{ij,kk}(x,y) + (\lambda+\mu)U_{kj,ki}(x,y) = -\delta_{ij}\delta(x-y) \tag{14}$$

i.e.

$u_i^*(x) = U_{ij}(x,y)e_j(y)$ and $t_i^*(x) = T_{ij}(x,y)e_j(y)$

with $e_j(y)$ being the unit orthogonal base vectors, one obtains the integral representation of the displacement field

$$\begin{aligned}u_i(y) &= \int_\Gamma U_{ij}(x-y)t_j(x)d\Gamma - \int_\Gamma T_{ij}(x,y)u_j(x)d\Gamma \\ &+ \int_\Gamma \gamma n_j(x)\theta(x)U_{ij}(x-y)d\Gamma \\ &- \int_\Omega [\gamma\theta_{,j}(x) - X_j(x)]U_{ij}(x-y)d\Omega\end{aligned} \tag{15}$$

The local boundary integral equation is considered on a subdomain Ω_s. On the artificial boundary $\partial\Omega_s$, both the displacement and traction vectors are unknown. In order to get rid of the traction vector in the integral over $\partial\Omega_s$, the concept of a '*companion solution*' can be utilized successfully [Atluri et al.(2000)]. The companion solution is associated with the fundamental solution U_{ij} and is defined as the solution to the following equations:

$$\tilde{\sigma}_{ij,j} = 0 \text{ on } \Omega_s'$$
$$\tilde{U}_{ij} = U_{ij} \text{ on } \partial\Omega_s' \tag{16}$$

where Ω_s' is a circle of radius r_0, which coincides with Ω_s for interior points. The modified test function $U_{ij}^* = U_{ij} - \tilde{U}_{ij}$ has to satisfy the governing equation (14). Then, the integral equation (15) is valid also for modified fundamental solution U_{ij}^*. On a circle $\partial\Omega_s'$, this fundamental solution is zero due to the second condition (16). Hence, we can write

$$u_i(y) = -\int_{\partial\Omega_s} T_{ij}^*(x,y)u_j(x)d\Gamma - \int_{\Omega_s}[\gamma\theta_{,j}(x) - X_j(x)]U_{ij}^*(x-y)d\Omega \tag{17}$$

for the source point y located inside Ω . The explicit expression for modified test function and modified fundamental traction T_{ij}^* one can find in [Atluri et al.(2000)]. For $\zeta \in \Gamma_s \subset \Gamma$ (source point located on the global boundary) the LBIE can be written as

$$\begin{aligned} u_i(\zeta) + \int_{L_s} T_{ij}^*(x,\zeta)u_j(x)d\Gamma + \lim_{y\to\zeta}\int_{\Gamma_s} T_{ij}^*(x,y)u_j(x)d\Gamma \\ - \int_{\Gamma_s}[t_j(x) + \gamma n_j(x)\theta(x)]U_{ij}^*(x-\zeta)d\Gamma = \\ - \int_{\Omega_s}[\gamma\theta_{,j}(x) - X_j(x)]U_{ij}^*(x-\zeta)d\Omega \end{aligned} \tag{18}$$

Next we will assume the body forces X_i to be zero. The domain integral on the right hand sides of eqs. (17) and (18) can be transformed to boundary integrals in the same way as presented in the book [Balas et al.(1989)]. Applying the Gauss divergence theorem to the domain integral in eq. (17) one can write

$$\begin{aligned} \gamma\int_{\Omega_s}\theta_{,j}(x)U_{ij}^*(x-y)d\Omega = \\ \gamma\int_{\partial\Omega_s}\theta(x)n_j(x)U_{ij}^*(x-y)d\Gamma - \gamma\int_{\Omega_s}\theta(x)U_{ij,j}^*(x-y)d\Omega \end{aligned} \tag{19}$$

In stationary thermoelasticity the following governing equations have to be satisfied [Balas et al.(1989)]

$$\begin{aligned} \mu U_{ij,kk}^* + (\lambda+\mu)U_{kj,ki}^* &= -\delta(r)\delta_{ij} \\ \mu V_{i,kk}' + (\lambda+\mu)V_{k,ki}' &= \gamma T_{,i} \\ T_{,ii} &= -\delta(r) \end{aligned} \tag{20}$$

where V_i' is the fundamental displacement corresponding to a point heat source (see the third equation in (20)). Differentiating the second equation in (20) by ∂_i one obtains

$$(\lambda+2\mu)\nabla^2 V_{i,i}' = \gamma T_{,ii} \tag{21}$$

From eq. (21) it follows directly

$$V_{i,i}' = \frac{\gamma}{\lambda+2\mu}T + A \tag{22}$$

where A is a harmonic function, i.e. $\nabla^2 A = 0$.

Substituting eq. (22) into the second equation of (20) one can write

$$\nabla^2 V_i' = \frac{\gamma}{\lambda+2\mu}T_{,i} - \frac{\lambda+\mu}{\mu}A_{,i} \tag{23}$$

Replacing the right hand side (Dirac delta function) in the first equation of (20) by the Laplacian of temperature (see the third equation) and differentiating according ∂_i, we obtain the following relation

$$(\lambda+2\mu)U_{ij,kki}^* = \nabla^2 T_{,i} \tag{24}$$

Now, replacing the gradient of temperature in (24) by the corresponding terms given by eq. (23) we get

$$(\lambda+2\mu)\nabla^2 U_{ij,i}^* = \nabla^2\left(\nabla^2 V_j'\frac{\lambda+2\mu}{\gamma} + \frac{\lambda+\mu}{\mu}\frac{\lambda+2\mu}{\gamma}A_{,j}\right) \tag{25}$$

Taking into account $\nabla^2 A_{,j} = 0$ we can write

$$U^*_{ij,i} + B_j = \frac{1}{\gamma}\nabla^2 V'_j \tag{26}$$

where B_j are harmonic functions, i.e. $\nabla^2 B_j = 0$.

Equation (26) can be rewritten into a more convenient form

$$U^*_{ij,i} = \frac{1}{\gamma}\nabla^2 V^*_j \tag{27}$$

where $V^*_j = V'_j - \tilde{V}_j$ and $\nabla^2 \tilde{V}_j = \gamma B_j$.

The analytic expression of V^*_j can be found in Appendix.

Substituting eq. (27) into the domain integral in eq. (19) and applying the Gauss divergence theorem we get

$$\gamma \int_{\Omega_s} \theta(x) U^*_{ij,j}(x-y)\,d\Omega = \int_{\partial\Omega_s} \theta(x) V^*_{i,j}(x-y) n_j(x)\,d\Gamma - \int_{\partial\Omega_s} \theta_{,j}(x) n_j(x) V^*_i(x-y)\,d\Gamma \tag{28}$$

Then, the pure boundary LBIE for an interior point can be written as

$$u_i(y) = -\int_{\partial\Omega_s} T^*_{ij}(x,y) u_j(x)\,d\Gamma + \int_{\partial\Omega_s} \theta(x) Z^*_i(x,y)\,d\Gamma - \int_{\partial\Omega_s} q(x) V^*_i(x-y)\,d\Gamma \tag{29}$$

where $Z^*_i = V^*_{i,j} n_j$ (see Appendix).

The alternative pure boundary integral equation for $\zeta \in \Gamma_s \subset \Gamma$ is given as

$$u_i(\zeta) + \int_{L_s} T^*_{ij}(x,\zeta) u_j(x)\,d\Gamma + \lim_{y\to\zeta} \int_{\Gamma_s} T^*_{ij}(x,y) u_j(x)\,d\Gamma - \int_{\Gamma_s} t_j(x) U^*_{ij}(x-\zeta)\,d\Gamma = \int_{\Omega_s} [\theta(x) Z^*_i(x-\zeta) - q(x) V^*_i(x-\zeta)]\,d\Omega \tag{30}$$

The LBIE (29) and (30) based on a pure boundary formulation are more convenient for numerical implementation than those with the domain integral given in eqs. (17) and (18).

4 Moving least squares approximation and discretization

The moving least squares (MLS) approximation is generally considered as one of schemes to interpolate data with a reasonable accuracy. Consider the approximation of a function $\mathbf{u}(\boldsymbol{x})$ in a domain Ω with a number scattered nodes $\{\mathbf{x}_i\}$, $i = 1, 2, ...n$, the MLS approximant $\mathbf{u}^h(\mathbf{x})$ of $\boldsymbol{u}$, $\forall \mathbf{x} \in \Omega$, can be defined by

$$\mathbf{u}^h(\mathbf{x}) = \mathbf{p}^T(\mathbf{x})\mathbf{a}(\mathbf{x}) \quad \forall \mathbf{x} \in \Omega \tag{31}$$

where $\mathbf{p}^T(\mathbf{x}) = [p_1(\mathbf{x}), p_2(\mathbf{x}), ..., p_m(\mathbf{x})]$ is a complete monomial basis of order m; and $\mathbf{a}(\mathbf{x})$ is a vector containing coefficients $a_j(\mathbf{x})$, $j = 1, 2, ..., m$ which are functions of the space co-ordinates $\mathbf{x} = [x, y, z]^T$. For example, for a 2-d problem:

$\mathbf{p}^T(\mathbf{x}) = [1, x, y]$, linear basis $m = 3$
$\mathbf{p}^T(\mathbf{x}) = \left[1,\ x,\ y,\ (x)^2,\ xy,\ (y)^2\right]$ quadratic basis $m = 6$.

The coefficient vector $\mathbf{a}(\mathbf{x})$ is obtained by performing a weighted least-squares fit for the local approximation

$$J(x) = \sum_{i=1}^{n} w_i(x) \left[\mathbf{p}^T(x_i)\mathbf{a}(\mathbf{x}) - \hat{u}_i\right]^2 = [\mathbf{P}\mathbf{a}(\mathbf{x}) - \hat{\mathbf{u}}]^T \mathbf{W} [\mathbf{P}\mathbf{a}(\mathbf{x}) - \hat{\mathbf{u}}] \tag{32}$$

where $w_i(\mathbf{x}) = w(\mathbf{x} - \mathbf{x}_i)$ is the weight function associated with the node i. The weight function $w(\mathbf{x} - \mathbf{x}_i)$ is defined as a monotonically decreasing function as the distance between the evaluation point and the node increases. Thus, the weight function can be parametrized by the distance $d_i = \|\mathbf{x} - \mathbf{x}_i\|$. In this paper, the weight function is the Gaussian weight function given by

$$w_i(\mathbf{x}) = \begin{cases} \dfrac{\exp\left[-(d_i/c_i)^2\right] - \exp\left[-(r_i/c_i)^2\right]}{1 - \exp\left[-(r_i/c_i)^2\right]} & 0 \le d_i \le r_i \\ 0 & d_i \ge r_i \end{cases}$$

(33)

where r_i is the radius of the domain of influence of the i node and c_i is a constant controlling the shape of the weight function w_i.

In eq. (32) $\hat{u}_i$ denotes the fictitious nodal values and not the nodal values of the unknown trial function in general. To find the coefficient $\mathbf{a}$, we perform the extremum of J by

$$\partial J/\partial \mathbf{a} = \mathbf{A}(\mathbf{x})\mathbf{a}(\mathbf{x}) - \mathbf{B}(\mathbf{x})\hat{\mathbf{u}} = 0 \tag{34}$$

where matrices $\mathbf{A}(\mathbf{x})$ and $\mathbf{B}(\mathbf{x})$ are defined:

$$\mathbf{A}(\mathbf{x}) = \mathbf{P^T W P} = \sum_{i=1}^{n} w_i(\mathbf{x})\mathbf{p}(\mathbf{x}_i)\mathbf{p}^T(\mathbf{x}_i)$$
$$\mathbf{B}(\mathbf{x}) = \mathbf{P^T W} = [w_1(\mathbf{x})\mathbf{p}(\mathbf{x}_1), w_2(\mathbf{x})\mathbf{p}(\mathbf{x}_2), ..., w_n(\mathbf{x})\mathbf{p}(\mathbf{x}_n)]$$

Solving this for $\mathbf{a}(x)$ and substituting it into eq. (31), we get

$$\mathbf{u}^h(\mathbf{x}) = \Phi^T(\mathbf{x}) \cdot \hat{\mathbf{u}} = \sum_{i=1}^{n} \phi_i(\mathbf{x})\hat{u}_i \tag{35}$$

where

$$\Phi^T(\mathbf{x}) = \mathbf{p}^T(\mathbf{x})\mathbf{A}^{-1}(\mathbf{x})\mathbf{B}(\mathbf{x}) \tag{36}$$

The partial derivatives of the MLS shape functions are obtained as

$$\phi_{i,k} = \sum_{j=1}^{m} \left[p_{j,k}(\mathbf{A}^{-1}\mathbf{B})_{ji} + p_j(\mathbf{A}^{-1}\mathbf{B}_{,k} + \mathbf{A}^{-1}_{,k}\mathbf{B})_{ji} \right] \tag{37}$$

It should be noted that the MLS approximation is well defined only when the matrix $\mathbf{A}$ in eq. (34) is non-singular. A necessary condition for a well-defined MLS approximation is that at least m weight functions are non-zero (i.e., $n \geq m$) for each sample point.

Substituting the MLS approximation (35) into the definition formula of traction vector, we get

$$\mathbf{t}(\mathbf{x}) = \mathbf{N}(\mathbf{x})\mathbf{D}\sum_{j=1}^{n} \mathbf{B}_j(\mathbf{x})\hat{u}_j - \boldsymbol{\gamma}\mathbf{n}\sum_{j=1}^{n} \phi_j(\mathbf{x})\hat{\theta}_j \tag{38}$$

where matrix $\mathbf{N}$ correspond to normal vector $\mathbf{n}$

$$\mathbf{N}(\mathbf{x}) = \begin{bmatrix} n_1 & 0 & n_2 \\ 0 & n_2 & n_1 \end{bmatrix}$$

the stress-strain matrix $\mathbf{D}$ is given by

$$\mathbf{D} = \frac{2\mu}{1-2\overline{\nu}} \begin{bmatrix} 1-\overline{\nu} & \overline{\nu} & 0 \\ \overline{\nu} & 1-\overline{\nu} & 0 \\ 0 & 0 & (1-2\overline{\nu})/2 \end{bmatrix}$$

with for plane strain problem; $\overline{\nu} = \nu/(1+\nu)$ for plane stress problem, and

$$\mathbf{B}_j(\mathbf{x}) = \begin{bmatrix} \phi_{j,1} & 0 \\ 0 & \phi_{j,2} \\ \phi_{j,2} & \phi_{j,1} \end{bmatrix}$$

Let $\Gamma_s = \Gamma_{su} \cup \Gamma_{st}$, where Γ_{su} and Γ_{st} are finite parts of Γ_s over which these (temperature and displacements) or (heat flux and tractions) are prescribed, respectively.

In view of the uncoupled theory and the use of the MLS-approximation, the discretized LBIE (10) and (11) collocated at $y_i \in \Omega$ and $\zeta_i \in \Gamma_{st}$ become

$$\sum_{j=1}^{n} \left\{ \phi_j(y_i) + \int_{\partial\Omega_s} \frac{\partial\tilde{\theta}^*}{\partial n}(x, y_i)\phi_j(x)d\Gamma \right\} \hat{\theta}_j = 0 \tag{39a}$$

$$\begin{aligned} &\sum_{j=1}^{n} \left\{ \phi_j(\zeta_i) + \int_{L_s} \frac{\partial\tilde{\theta}^*}{\partial n}(x, \zeta_i)\phi_j(x)d\Gamma \right\} \hat{\theta}_j \\ &+ \sum_{j=1}^{n} \lim_{y\to\zeta_i} \int_{\Gamma_{st}} \frac{\partial\tilde{\theta}^*}{\partial n}(x, y)\phi_j(x)d\Gamma\hat{\theta}_j - \\ &- \sum_{j=1}^{n} \int_{\Gamma_{su}} \tilde{\theta}^*(x, \zeta_i)\left[n_1\phi_{j,1}(x) + n_2\phi_{j,2}(x)\right]d\Gamma\hat{\theta}_j \\ &= \int_{\Gamma_{st}} \tilde{\theta}^*(x, \zeta_i)\overline{q}(x)d\Gamma - \int_{\Gamma_{su}} \frac{\partial\tilde{\theta}^*}{\partial n}(x, \zeta_i)\overline{\theta}(x)d\Gamma \end{aligned} \tag{39b}$$

The set of algebraic equations (39a) and (39b) should be supplemented by the equations

$$\sum_{j=1}^{n} \phi_j(\zeta_i)\hat{\theta}_j = \overline{\theta}(\zeta_i) \quad , \quad \zeta_i \in \Gamma_{su} \tag{39c}$$

in order to get a complete set for computation of the fictitious unknowns $\hat{\theta}_j$ at all the nodal points.

Having known the thermal fields, we can calculate the fictitious unknowns $\hat{u}_j$. The discretized LBIE (29) and (30) collocated at $y_i \in \Omega$ and $\zeta_i \in \Gamma_{st}$ become

$$\sum_{j=1}^{n} \left\{ \phi_j(y_i) + \int_{\partial\Omega_s} \mathbf{T}^*(\mathrm{x},\mathrm{y_i})\phi_\mathrm{j}(\mathrm{x})\mathrm{d}\Gamma \right\} \hat{u}_j =$$
$$\sum_{j=1}^{n} \hat{\theta}_j \int_{\partial\Omega_s} \left[\mathbf{Z}^*(\mathrm{x},\mathrm{y_i})\phi_\mathrm{j}(\mathrm{x}) - \mathbf{V}^*(\mathrm{x},\mathrm{y_i}) \left(\mathrm{n_1}\phi_{\mathrm{j},1}(\mathrm{x}) - \mathrm{n_2}\phi_{\mathrm{j},2}(\mathrm{x}) \right) \right] d\Gamma \tag{40a}$$

$$\begin{aligned}
&\sum_{j=1}^{n} \phi_j(\zeta_i)\hat{u}_j + \sum_{j=1}^{n} \int_{L_s} \mathbf{T}^*(x,\zeta_i)\phi_j(x)d\Gamma\,\hat{u}_j \\
&\quad + \sum_{j=1}^{n} \lim_{y\to\zeta_i} \int_{\Gamma_{st}} \mathbf{T}^*(x,y)\phi_j(x)d\Gamma\,\hat{u}_j \\
&\quad - \sum_{j=1}^{n} \int_{\Gamma_{su}} \mathbf{U}^*(x,\zeta_i)\mathbf{N}(x)\mathbf{D}\mathbf{B}_j(x)d\Gamma\,\hat{u}_j = \\
&\quad \int_{\Gamma_{st}} \mathbf{U}^*(x,\zeta_i)\overline{\mathbf{t}}(x)d\Gamma - \int_{\Gamma_{su}} \mathbf{T}^*(x,\zeta_i)\overline{\mathbf{u}}(x)d\Gamma \\
&\quad \int_{\Gamma_{su}} \mathbf{Z}^*(x,\zeta_i)\overline{\theta}(x)d\Gamma - \int_{\Gamma_{st}} \mathbf{V}^*(x,\zeta_i)\overline{q}(x)d\Gamma \\
&+ \sum_{j=1}^{n} \hat{\theta}_j \int_{L_s\cup\Gamma_{st}} [\mathbf{Z}^*(x,\zeta_i)\phi_j(x) - \mathbf{V}^*(x,\zeta_i)(n_1\phi_{j,1}(x) - n_2\phi_{j,2}(x))]d\Gamma
\end{aligned} \tag{40b}$$

where the matrix notations $\mathbf{U}^*$, $\mathbf{T}^*$, $\mathbf{V}^*$ and are used instead of the tensor notations U^*_{ij}, T^*_{ij}, U^*_i and Z^*_i, respectively.

Finally, the set of equations (40a) and (40b) is supplemented by the equations

$$\sum_{j=1}^{n} \phi_j(\zeta_i)\hat{u}_j = \overline{\mathbf{u}}(\zeta_i) \quad \zeta_i \in \Gamma_{su} \tag{40c}$$

Now, the fictitious unknowns $\hat{u}_j$ can be calculated by solving the set of algebraic equations (40). The limit of the singular integral over Γ_{st} can be evaluated numerically, by using a regular quadrature accurately, provided that an optimal transformation of the integration variable is employed before the integration [Sladek et al.(2000)].

5 Numerical examples

In this section numerical results will be presented to test the accuracy of the present computational method.

5.1 Patch test

Consider the material in a quadrilateral cross-section $(2a \times 2a)$ subjected to a uniform thermal load θ and fixed displacements in x_2- and x_3- directions (see Fig. 1). The following material constants are assumed: Young modulus $E = 1.0 \bullet 10^5\,\mathrm{MPa}$, Poisson ratio $\nu = 0.25$ and coefficient of thermal expansion $\alpha = 1.0 \bullet 10^{-5}\,\mathrm{deg}^{-1}$. If the bar subjected to a uniform thermal load is fixed in x_3- direction (plane strain conditions are assumed) the strain tensor ε^t_{22} is given as

$$\varepsilon^t_{22} = (1+\nu)\alpha\theta$$

The thermal strain tensor ε^t_{22} has to be eliminated by the mechanical strain ε^m_{22} due to the fixed displacement in x_2- direction. For a uniform load $\sigma_{22}(x_1) = p$ of a square patch the displacement vector under plane strain conditions are:

$$u^m_1 = -\nu(1+\nu)\frac{p}{E}x_1$$

$$u^m_2 = (1-\nu^2)\frac{p}{E}x_2$$

Then, the analytical expression for the stress σ_{22} in the patch under a uniform thermal load with fixed displacements in x_2- and x_3- directions can be written as

$$\sigma_{22} = p = -(1+\nu)\frac{\alpha E\theta}{1-\nu^2} \quad . \tag{41}$$

Owing to the symmetry, it is sufficient to analyse only a quarter of the cross section. In meshless LBIE analysis we have selected 16 nodes with an equidistant distribution on the boundary of the analysed domain. To

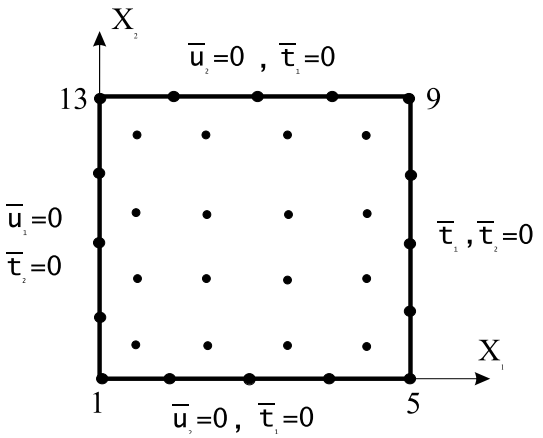

Figure 1 : Square patch under a uniform temperature load

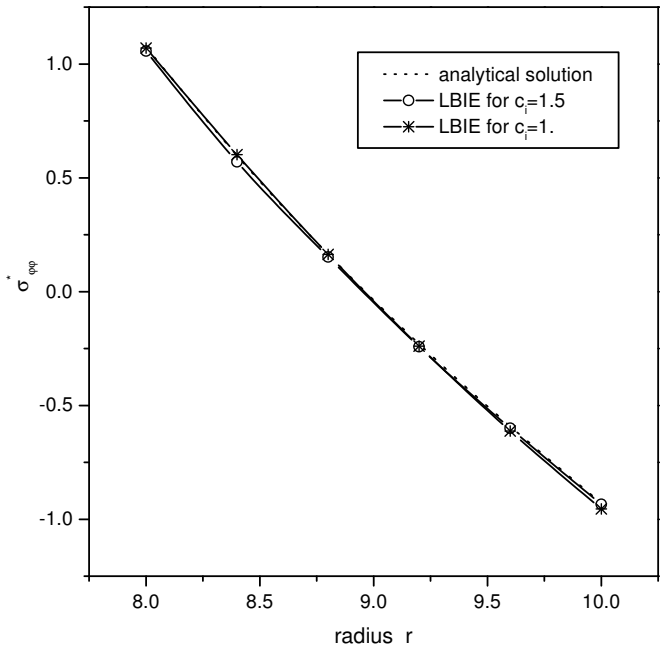

Figure 2 : Comparison of numerical errors for stresses σ_{22} at internal points lying on $x_2 = 0.5$ line

boundary nodes, 16 additional interior nodes are considered (Fig. 1). The radii of circular subdomains were constant $r_{loc} = 0.6$ for boundary nodes and $r_{loc} = 0.4$ for interior nodes. We have also considered $c_i = 1$ and $r_i/c_i = 4$ in the Gaussian weight function.

To compare the accuracy of the numerical results for stresses σ_{22} obtained by the LBIE method with the other numerical method, we have analysed the same boundary value problem by the conventional boundary element method based on the pure boundary integral equation formulation [Balas et al.(1989)]. For discretization of boundary we have used 8 quadratic elements. It is known that accuracy of the numerical results in the conventional BIE method is decreasing at points, which are close to the boundary provided that no special treatment of nearly-singular integrals is adopted in the numerical integration. For comparison of numerical results we have made analyses at points, which are on the line.

The dependence of the traction norm error, defined as $x_2 = 0.5$. The shortest distance such points from the boundary, s, is equal or lower than 0.5 . Then, the ratio of s to the element length d is $s/d \leq 0.25$. In Fig. 2 one can see that the lowest accuracy for the BIE results is at points which have the shortest distance to the mid-node of boundary element. The accuracy is changing from 0.2% to 2.1% . On the other hand, the LBIE method yields the accuracy 0.05% at all the points of observation.

The relative error (accuracy) is defined as

$$r = \frac{|\sigma_{22} - \sigma_{22}^{exact}|}{|\sigma_{22}^{exact}|}[\%]$$

where σ_{22}^{exact} is taken from eq. (41).

5.2 *Hollow cylinder*

To compare the accuracy of the proposed numerical scheme with analytical results, we present an example of the computation of the radial distribution of the temperature and stresses in a hollow cylinder subjected to a thermal gradient. On internal and external surfaces of the hollow cylinder different, but constant temperatures are prescribed (Fig. 3). Because of the symmetry of the problem, it is sufficient to analyse only a quarter of the cylinder.

Analytical distributions of temperature and hoop stresses are given by

$$\theta(r) = \theta_1 + \frac{\Delta\theta}{\ln R_2/R_1} \ln r^*$$

$$\sigma_{\varphi\varphi} = \Delta\theta \frac{E\alpha}{2(1-\nu)} \left[\frac{1+(1/r^*)^2}{1-(R_1/R_2)^2} + \frac{1+\ln r^*}{\ln R_1/R_2} \right] \qquad (42)$$

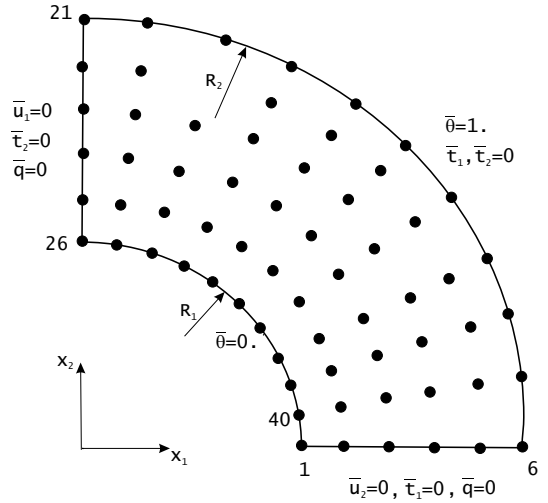

Figure 3 : Nodes for the hollow cylinder subject to thermal load

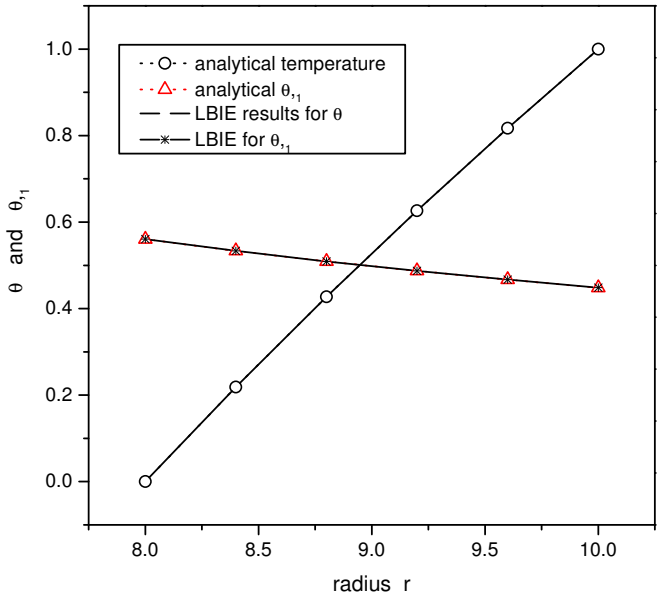

Figure 4 : Temperature and temperature gradient along x_1- coordinate

where $r^* = r/R_1$ and $\Delta\theta = \theta_2 - \theta_1$.

In the numerical analysis we have considered the following geometrical and material constants: cylinder radii $R_1 = 8$, $R_2 = 10$; Young modulus $E = 2.0 \bullet 10^5$ MPa; Poisson ratio $\nu = 0.25$ and coefficient of thermal expansion $\alpha = 1.67 \bullet 10^{-5}$ deg^{-1}. We have used 40 nodes on the boundary and 56 additional interior nodes. On both artificial cuts (due to symmetry) the radii of subdomains are constant $r_{loc} = 0.39$. On the rest part of the boundary (curvilinear surfaces) the size of subdomains is constant too, $r_{loc} = 0.49$. Next, $c_i = 1.5$ and $r_i/c_i = 4$ are considered.

Numerical results for temperature and temperature gradient obtained by the LBIE method are compared with analytical ones in Fig. 4. One can see an excellent agreement. The relative error for temperature in the whole radius interval is less than 0.001% and for temperature gradient is less than 0.05% .

The hoop stresses are normalized to obtain a non-dimensional value according the formula

$$\sigma^*_{\varphi\varphi} = \frac{2(1-\nu)}{\Delta\theta E\alpha}\sigma_{\varphi\varphi}$$

The distribution of the non-dimensional $\sigma^*_{\varphi\varphi}$ along the radius of the hollow cylinder is shown in Fig. 5. One can observe a quite good agreement of analytical results with LBIE ones. Various values of the weight function parameter c_i at the constant size of the support domain $r_i = 6$ were considered in the numerical analysis. The relative errors for the hoop stresses on internal and external surfaces of the hollow cylinder are defined as

$$r_I = \frac{\left|\sigma_{\varphi\varphi}(R_I) - \sigma^{exact}_{\varphi\varphi}(R_I)\right|}{\left|\sigma^{exact}_{\varphi\varphi}(R_I)\right|}[\%] \quad \text{for } I = 1, 2 \ .$$

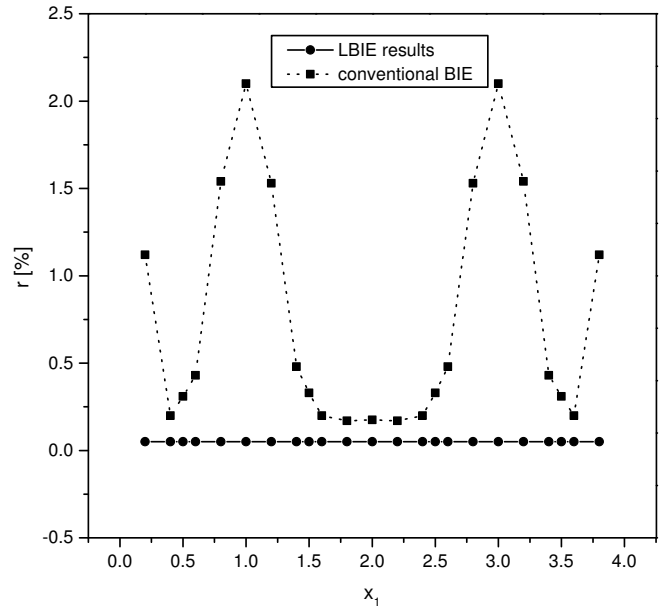

Figure 5 : Hoop stress distribution along the radius of the hollow cylinder

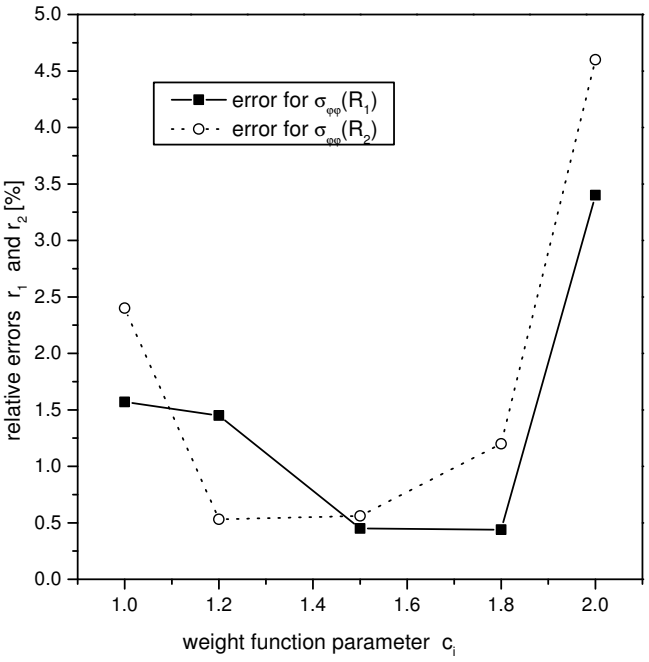

Figure 6 : Dependence of relative errors for hoop stresses on the weight function parameter c_i

Figure 6 shows the influence of the weight function parameter c_i on the accuracy of hoop stresses for both cylinder surfaces. Accuracy on the whole c_i interval is higher than 5% . Even for optimal of c_i the accuracy is higher than 1% .

6 Conclusion

The local boundary integral equation (LBIE) method with a meshless approximation has been applied successfully, to solve 2-d boundary value problems in stationary thermoelasticity. The moving least square method is used for approximation of physical quantities. Pure contour boundary integral equations, with circular subdomains, have been utilized as LBIE. Introducing the modified fundamental solution for displacement, which gives zero displacement values on the contour of the subdomain, we eliminate the traction quantity from the local boundary integral equations. The modified fundamental solution requires one to derive new corresponding fundamental solutions related to a point heat source. They are used to develop a pure contour local boundary integral formulation in stationary thermoelasticity. The suggested method is computionally efficient, due to the missing domain integration.

A variety of numerical experiments have been carried out, to optimalize the size of support domain r_i and the weight function parameter c_i. It follows from the analyses that ratio $r_i/c_i = 4$ is the most optimal. The well-known boundary layer effect (lost accuracy of results at points close to the boundary) for conventional BIE does not arise in the LBIE with the MLS approximation. In such a case, the accuracy does not dependent on the position of an evaluation point. It is a great advantage of suggested method.

Appendix

In this Appendix we derive the explicit expression for modified fundamental displacement corresponding to a point heat source, U_j^*. The fundamental displacement has to satisfy eq. (27). The modified test function U_{ij}^* is given by [Atluri et al.(2000)]

$$U_{ij}^* = U_{ij} - \tilde{U}_{ij} \tag{43}$$

where

$$U_{ij} = \frac{1}{8\pi\mu(1-\overline{\nu})}[(4\overline{\nu}-3)\ln r\delta_{ij} + r_{,i}r_{,j}] \tag{44}$$

$$\tilde{U}_{ij} = \frac{1}{8\pi\mu(1-\overline{\nu})}\left\{\left[(4\overline{\nu}-3)\ln r_0 + \frac{5-4\overline{\nu}}{2(3-4\overline{\nu})}\left(1-\frac{r^2}{r_0^2}\right)\right]\delta_{ij} + \frac{r_i r_j}{r_0^2}\right\} \tag{45}$$

and r_0 is the radius of the circular subdomain Ω_s.

Considering eq. (43) we can rewrite eq. (27) into the form

$$U_{ij,i} - \tilde{U}_{ij,i} = \frac{1}{\gamma}\nabla^2(V_j' - \tilde{V}_j) \tag{46}$$

From (45) it follows directly

$$\tilde{U}_{ij,i} = \frac{1-2\overline{\nu}}{3-4\overline{\nu}}\frac{1}{2\pi\mu(1-\overline{\nu})}\frac{rr_{,j}}{r_0^2} \tag{47}$$

Thus, the additional fundamental displacement $\tilde{V}_j$ has to satisfy the following equation

$$\nabla^2 \tilde{V}_j = \frac{1-2\overline{\nu}}{3-4\overline{\nu}} \frac{\gamma}{2\pi\mu(1-\overline{\nu})} \frac{r_j}{r_0^2} \tag{48}$$

It can be easy shown that function

$$\tilde{V}_j = \frac{1-2\overline{\nu}}{3-4\overline{\nu}} \frac{\gamma}{16\pi\mu(1-\overline{\nu})} \left(\frac{r}{r_0}\right)^2 r_j \tag{49}$$

satisfies eq. (48).

The analytic expression of V_j' is given in (Balas et al., 1989). Finally, we can write

$$V_j^* = -\frac{m}{8\pi} r_j (1+2\ln r) - \frac{m}{8\pi} \frac{r^2 r_j}{(3-4\overline{\nu}) r_0^2} \tag{50}$$

where

$$m = \frac{\gamma}{\lambda+2\mu} = \frac{\gamma}{2\mu} \frac{1-2\overline{\nu}}{1-\overline{\nu}}$$

From (50) one can obtain

$$Z_j^* = V_{j,i}^* n_i =$$
$$-\frac{m}{8\pi}[(1+2\ln r) n_j + 2 r_{,j} n_i r_{,i}] - \frac{m}{8\pi} \frac{(2 r_i n_i r_j + r^2 n_j)}{r_0^2 (3-4\overline{\nu})} \tag{51}$$

References

Atluri S.N., Sladek V., Sladek J. and Zhu T. (2000) The local boundary integral equation (LBIE) and its meshless implementation for linear elasticity. *Comput. Mech.* 25: 180-198.

Balas J., Sladek J. and Sladek V. (1989) Stress Analysis by Boundary Element Methods, Elsevier, Amsterdam

Belytschko T., Lu Y.Y. and Gu L. (1994) Element-free Galerkin methods. *Int. J. Num. Meth. Engn.* 37: 229-256.

Belytschko T., Krongauz Y., Organ D., Fleming M. and Krysl P. (1996) Meshless methods; An overview and recent developments. *Comp. Meth. Appl. Mech. Engn.*. 139: 3-47.

Ching, H.K., and Batra, R.C.(2001) Determination od Crack Tip Fields in Linear Elastostatics by Meshless Local Petrov-Galerkin (MLPG) Method. *CMES: Computer Modeling in Engineering & Sciences* Vol. 2, No. 2, pp 273-290.

Gu, Y.T. and Liu, G.R.(2001) A Meshless Local Petrov-Galerkin (MLPG) Formulation for Static and Free Vibration Analyses of Thin Plates. *CMES: Computer Modeling in Engineering & Sciences* Vol. 2, No. 4, pp 463-476.

Kim, H.G. and Atluri, S.N.(2000) Arbitrary Placement of Secondary Nodes and Error Control in the Meshless Local Petrov-Galerkin (MLPG) Method. *CMES: Computer Modeling in Engineering & Sciences* Vol. 1, No. 3, 11-32.

Lin, H. and Atluri, S.N.(2000) Meshless Local Petrov-Galerkin (MLPG) Method for Convection-Diffusion Problems. *CMES: Computer Modeling in Engineering & Sciences* Vol. 1, No. 2, 45-60

Sladek V., Sladek, J., Atluri S.N. and Van Kerr, R. (2000) Numerical integration of singularities in a meshless implementation of local boundary integral equations. *Comput. Mech.* 25: 394-403.

Zhu T., Zhang J.D. and Atluri S.N. (1998) A local boundary integral equation (LBIE) method in computational mechanics, and a meshless discretization approach. *Comput. Mech.* 21: 223-235.